Structure and properties of amorphous gallium arsenide by tight-binding molecular dynamics

C. Molteni, L. Colombo, and L. Miglio
Dipartimento di Fisica, Università di Milano, via Celoria 16, 20133 Milano, Italy
(Received 23 March 1994)

We present and discuss the room-temperature structural, vibrational, and electronic properties of *a*-GaAs, as obtained by a tight-binding molecular-dynamics quenching of the liquid from 1600 K. An interesting comparison is also made with the overcooled liquid at 800 K, where solidlike and liquidlike features do coexist. At variance with previous *ab initio* calculations, we have been able to produce a good amorphous sample without introducing *ad hoc* moves of atoms, favoring a preselected distribution of point defects. Our results are in rather good agreement with the overall structural properties of *a*-GaAs, as deduced from experiments, and provide a detailed microscopic characterization of such a material.

I. INTRODUCTION

Amorphous GaAs (*a*-GaAs) has been the subject of intense experimental[1-6] and theoretical[7-9] research, mainly devoted to characterizing its short-range order (SRO) properties which, however, are still a matter of discussion. In particular, two main issues must be clarified: (i) a full characterization of the topological and chemical disorder of the amorphous network and (ii) the identification of structural point defects (like dangling or floating bonds) due to the presence of threefold- and fivefold-coordinated sites in the amorphous network.

In the present work we apply a molecular-dynamics scheme,[10] which provides the structural, electronic, and vibrational properties of *a*-GaAs at room temperature. In our scheme, the forces governing the atomic motion explicitly include the contribution of the electronic structure of the sample, as calculated through a semiempirical tight-binding (TB) method. A similar TB molecular dynamics[11] (TBMD) has been satisfactorily applied to elemental semiconductors [*l*-Si (Refs. 12 and 13) and *a*-Si (Refs. 14 and 15)]. However, no successful attempts to extend this method to III-V compounds were obtained up to now, due to the need for a suitable inclusion of charge-transfer effects.[10] The computational workload of TBMD is in between classical MD and self-consistent quantum-mechanical simulations, so that, even retaining the electronic information for each configuration, large-scale simulations involving hundreds of atoms and/or long times (hundreds of picoseconds) are possible.

It has been recently demonstrated[14] that the SRO features of an amorphous semiconductor obtained in a computer experiment are affected by the sample preparation. Consequently, two key points of the present work are the procedure adopted to prepare the *a*-GaAs sample and the careful monitoring of the slow quenching process from the liquid to the solid. Taking full advantage of the low computational cost of the TBMD simulation, we have been able to cool a good sample of *l*-GaAs (Refs. 10, 16, and 17) from 1600 down to 300 K, at an *average* cooling rate of 2.7×10^{12} K/s. Computationally speaking this is a very slow quenching rate, which allows us to avoid any artificial procedure in recovering the partial chemical order of the condensed phase, which is not observed in the liquid sample. The resulting amorphous network displays global structural properties in rather good agreement to the experiments.[1,2]

The reliability of the present simulation scheme is also confirmed by the study of the electronic properties of *a*-GaAs. We will show that the liquid-to-solid transition has driven GaAs from a metallic liquid to a solid semiconductor, in good agreement with previous first-principles calculations.[9] Finally, we have calculated the vibrational properties of *a*-GaAs and compared them to the crystal case.

The paper is organized as follows: in Sec. II we briefly present the TBMD model and describe the procedure for sample preparation. Details about the MD simulation are also included. In Sec. III we analyze the structural, electronic, and vibrational properties of the overcooled liquid at 800 K, in order to check the liquid-to-solid transition. In Sec. IV we present our results for *a*-GaAs and make a comparison to experimental data and first-principles calculations.

II. COMPUTATIONAL FRAMEWORK

In the TBMD approach, the time evolution of the atoms is obtained from the following Hamiltonian:[9]

$$H=\sum_i \frac{p_i^2}{2m_i}+2\sum_{\mathbf{k},n}^{\text{occ}}\epsilon_n(\mathbf{k})+U_{\text{rep}}\ , \tag{1}$$

where the energies $\epsilon_n(\mathbf{k})$ of the single-particle occupied states are obtained by diagonalizing a semiempirical TB matrix. Their sum is called band-structure energy E_{bs},[18] and provides the attractive covalent contribution to the total potential energy. In order to keep the computational cost as low as possible, in the present work we made use of the sp^3s^* basis set, which provides a good electronic density of states (DOS) without introducing second-neighbors interactions or more. The Koster-Slater hopping parameters (two-center approximation[19]) have been taken from Ref. 20 and their scaling upon the interatomic

distance has been chosen according to the Harrison rule.[19]

The last term in Eq. (1) takes into account all the repulsive contributions not included in the TB calculation, i.e., quantum-mechanical repulsion of the occupied orbitals and intra-atomic Coulombic repulsion due to site accumulation of electronic charge. In Ref. 10 we demonstrated that $U_{\rm rep}$ can be represented in terms of two-body contributions, that we cast in the following form:

$$U_{\rm rep}=\sum_{i,j>i}\left[\Phi_1\exp\left[-\frac{(r_{ij}-r_0)}{\alpha}\right]+\Phi_2\frac{r_0}{r_{ij}}\right], \qquad (2)$$

where r_{ij} is the relative distance between atom i and j, r_0 is its equilibrium value in the ZnS phase, and Φ_1, Φ_2, and α are fitting parameters to be determined. The first Born-Mayer term mainly describes the interatomic distance dependence of sp^3s^* orthogonality effects not included in the diagonal elements of the TB matrix.[10,21] On the other hand, $\Phi_2 r_0/r_{ij}$ takes into account the repulsion originated by a balance of Madelung attraction and Hartree repulsion, when charge-transfer effects are considered, as suggested by Ref. 21. The overall potential is weakly dependent on the interatomic distances, still linearly dependent on the coordination number inside the cutoff sphere as extensively discussed in Ref. 10. Φ_1, Φ_2, and α have been fitted onto the equilibrium lattice parameters and the difference in the equilibrium cohesive energies of the ZnS and NaCl crystalline phases of GaAs, as calculated at zero temperature by first principles.[22] Their values are 2.3906 eV, 1.2347 eV, and 0.3555 Å, respectively.

For what concerns like-atom interactions (required to handle the liquid phase from which we obtain the amorphous sample), we assumed that the repulsive interactions were the same as Eq. (2) (same parameters also, since Ga and As have nearly the same covalent radius), while the TB hopping parameters were taken from Ref. 7. In Table I we summarize the TB model parameters entering in this work. The accuracy of the present TBMD approach has been proven in Ref. 10 by studying l-GaAs, where both structural and electronic properties have been predicted in good agreement to experimental data[17] and first-principles simulations.[16] It is worth stressing that no adjustment of the TB and repulsive potential parameters has been performed during the simulation.

The amorphous sample was obtained by quenching a metallic liquid sample from 1600 down to 300 K through direct rescaling of the atomic velocities. The liquid-to-solid transition was divided in three steps: (i) cooling from 1600 to 800 K with an average rate of 3.08×10^{12} K/s, (ii) observation of the system for 20 ps at fixed temperature $T=800$ K, (iii) cooling from 800 to 300 K at a constant rate of 2.5×10^{12} K/s. This intermediate step was intended to check the structural properties of the sample, to monitor the liquid-to-solid transition, and to verify whether the structural, vibrational, and electronic properties of the sample were coherently approaching a solidlike behavior. During the quenching, the density of the sample was scaled linearly with the temperature, from the experimental value for the liquid ($\rho=5.71$ g/cm^3) to the one of the solid ($\rho=5.32$ g/cm^3). The equations of motion were integrated using a velocity-Verlet algorithm with a time step as large as 10^{-14} s. Despite this large time step, the total energy was conserved within 10^{-3} eV/atom.

TABLE I. Tight-binding parameters used in the present work.

	Ga-Ga	Ga-As	As-As
E_s	−2.656	−2.656(Ga)−8.343(As)	−8.343
E_p	3.669	3.669(Ga)1.041(As)	1.041
E_{s^*}	6.739	6.739(Ga)8.591(As)	8.591
V_{ss}	−2.0	−1.613	−1.42
V_{sp}	2.1	2.504(Ga)1.940(As)	2.1
$V_{pp}(\sigma)$	2.2	3.028	3.1
$V_{pp}(\pi)$	−0.67	−0.781	−0.79
V_{s^*p}	2.0	2.082(Ga)2.097(As)	1.8

The cooling process here imposed is quite computer demanding and can be realized by limiting the supercell size to 64 atoms (with periodic boundary conditions). This was enough to perform simulations as long as several hundred picoseconds thanks to a combination of (i) the reduced workload of the semiempirical TBMD scheme when compared to first-principles calculations, and (ii) the use of a very large time step due to the fact that the electronic degrees of freedom do not explicitly enter in the dynamics. We believe that a slow cooling process is an important feature of the present simulation; in fact, we have neither combined the MD simulation to Monte Carlo "moves" (as suggested in Ref. 23), nor applied "educated guesses" for Ga-As switches (as described in Ref. 9) in order to favor the formation of an amorphous network with specific topology and point-defect distribution.

After the cooling process, the sample was equilibrated during a constant-temperature constant-volume run for 90 ps and finally observed for 50 ps. The cutoff for the interactions was fixed to 3.185 Å, as in the case of l-GaAs.[15]

III. MONITORING THE LIQUID-TO-SOLID TRANSITION

In the top panels of Fig. 1, we show the total pair-correlation function $g(r)$ of l-GaAs (Ref. 10) at $T=1600$ K (left panel), the one of the sample at $T=800$ K (center panel), and the one of a-GaAs at $T=300$ K (right panel). In the center panel, the peak corresponding to the shell of second neighbors is clearly visible. This feature indicates that at $T=800$ K, short-range coordination beyond first neighbors is occurring even if $g(r)$ shows a minimum at ~3 Å, as is the case of l-GaAs. Anyway, the tendency to recover the chemical order of the solid phase is also demonstrated by the partial pair-correlation functions, as reported in the bottom panels of Fig. 1. Here we observe that like atoms mainly coordinate each other in second-neighbor positions, like in a crystal lattice, and that the corresponding interatomic distance between anions is larger than the one for cations.

In Fig. 2 (top, center, and bottom panels), we report

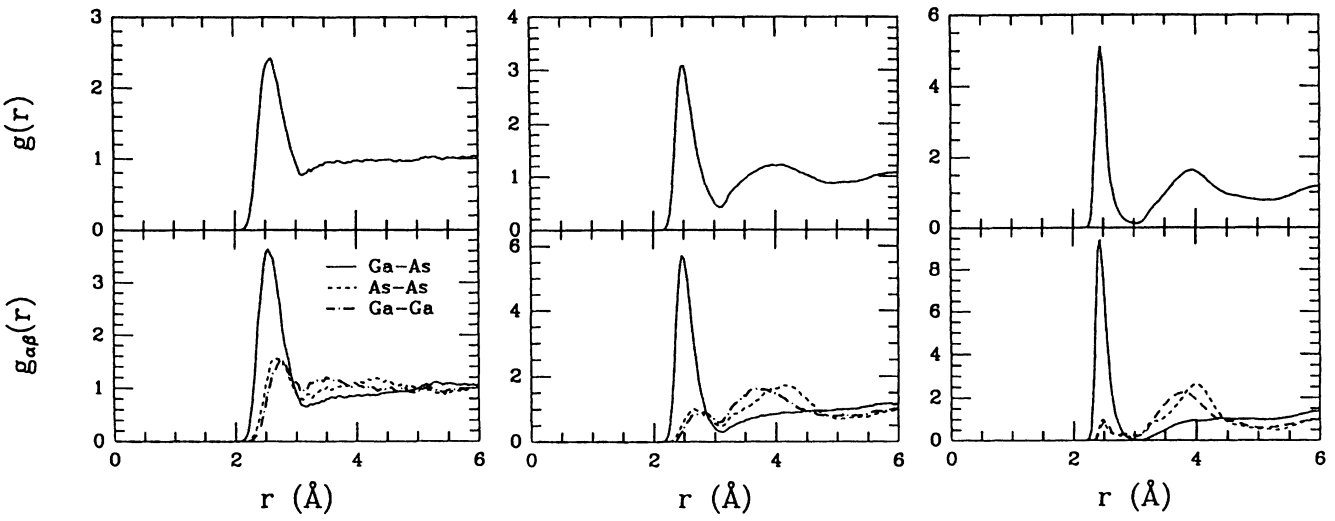

FIG. 1. Total (top) and partial (bottom) pair-correlation functions for GaAs at 1600 K (*l*-GaAs, left panel), at 800 K (center panel), and at 300 K (*a*-GaAs, right panel).

the coordination functions of *l*-GaAs (Ref. 10) at $T=1600$ K, the sample at $T=800$ K, and *a*-GaAs at $T=300$ K, respectively. We note that the distribution at $T=800$ K is strongly asymmetric, still resembling the liquid case. The average coordination number of our sample has decreased from 5.99 ($T=1600$ K) to 5.13 ($T=800$ K), still far from 4.08, the value corresponding to $T=300$ K. Moreover, the percentage of wrong bonds (i.e., bonds between like atoms) is sizable; it amounts to 24.11%.

By inspection of Fig. 3, we note that also the bond-angle distribution of the $T=800$ K sample (center panel) is more similar to a liquid (top panel) than to a solid (bottom panel), since the peak at 60° is still remarkable and the distribution strongly asymmetric.

As for the electronic properties, we have calculated both the total and site-projected DOS. The total DOS's are compared in Fig. 4 (top panels); here we see that at $T=800$ K we already have a remarkable definition of different electronic structures. The metallic character of the liquid phase is going to be lost and a deep minimum is appearing at the Fermi level. The site-projected DOS's (center and bottom part of Fig. 4) give more information about the occupation of the orbital states and show how the energy level corresponding to different angular momentum is less dispersed in energy than in *l*-GaAs.[24]

Finally, the vibrational spectra (Fig. 5), as calculated by Fourier transforming the velocity-velocity correlation functions, do confirm the qualitative results of Fig. 4; at $T=800$ K (center panel), we already have frequency separation between acoustic and optical structures, as for the solid. However, the density of modes at zero frequency is still high, typical of the liquid state and, by plotting the atomic mean-square atomic displacements (not here shown), we see that both anions and cations display a diffusive behavior.

All of the above information originates a complex picture in which liquidlike features coexist with solidlike ones. Our qualitative analysis indicates that our sample is really on the way to the amorphous state, but it is still at $T=800$ K an overcooled liquid (the experimental melting temperature for GaAs is $T=1511$ K). According to that, we have cooled the sample down to the solid phase ($T=300$ K) at a very slow rate. In other words, we have allowed the slow interdiffusion dynamics phenomena to recover the structure, the chemical order, and the semiconductive character of *a*-GaAs.

IV. THE AMORPHOUS STATE AT ROOM TEMPERATURE

The structure, which we obtained by a further quenching to room temperature, has been found to reproduce

TABLE II. Structural parameters for *a*-GaAs at $T=300$ K.

Pair	n[a]	d (Å)[a]	$\bar{\theta}$[a]	n[b]	d (Å)[b]	$\bar{\theta}$[b]	n[c]	d (Å)[c,d,e]	$\bar{\theta}$[c]
Ga-As	3.56	2.44		3.45	2.44				
Ga-Ga	0.53	2.37		0.38	2.39				
As-As	0.53	2.51		0.38	2.42				
All	4.09	2.44	106.7	3.83	2.44	108.2	3.93	2.48,[c] 2.51,[d] 2.46[e]	109

[a]Present work.
[b]Reference 9.
[c]Reference 1.
[d]Reference 2.
[e]Reference 3.

very closely a tetrahedral network. In fact, by considering the maximum first nearest-neighbor (1NN) distance as the one at which the first minimum of the pair-correlation function occurs (~ 3 Å in Fig. 1, right panel), we found an average coordination number $\bar{n}$ as large as 4.09, in good agreement with the experimental value which is 3.93.[1] The present value for $\bar{n}$ is larger than that calculated in Ref. 9 where, however, a smaller 1NN distance (2.8 Å) has been used. By inspection of Fig. 2 (bottom panel), we notice how the coordination distribution is remarkably symmetrical and less dispersed around $n=4$.

The tetrahedral character of the a-GaAs network is confirmed by the total bond-angle-distribution function $g(\theta)$ in Fig. 3 [bottom panel (a)]. There, the main structure falls at $\sim 106.7°$ in rather good agreement with the 109° experimental value.[1] The minor peak close to 60° is related to those bonds linking atoms whose relative distance falls in between the first maximum (~ 2.45 Å) and the first minimum (~ 3 Å) of the pair-correlation function. As already shown in the case of a-Si,[14] the intensity of such a shoulder is affected by the definition of the 1NN distance, which is in turn determined by the shape of $g(r)$.

In Table II we report the complete set of structural parameters for a-GaAs as obtained in the present computer experiment and compare them to the results of Ref. 9. In Table III we show the partial coordination numbers calculated with different cutoffs along with experimental and first-principles data.

More direct information about the microscopic ordering of a-GaAs come out from the partial $g(\theta)$ shown in

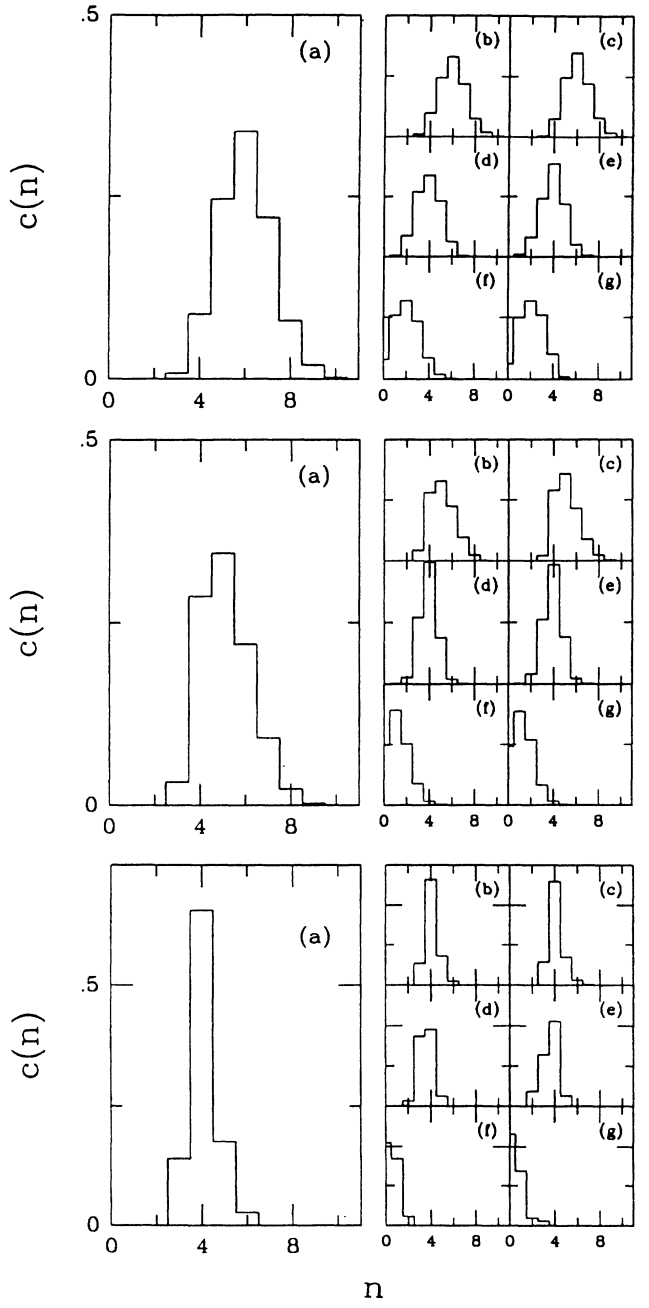

FIG. 2. Total (a) and partial coordination functions for GaAs at 1600 K (l-GaAs, top panel), at 800 K (center panel), and at 300 K (a-GaAs, bottom panel); (b) Ga-X (probability for a Ga atom to have n first neighbors of type X = Ga,As); (c) As-X; (d) Ga-As; (e) As-Ga; (f) Ga-Ga; (g) As-As.

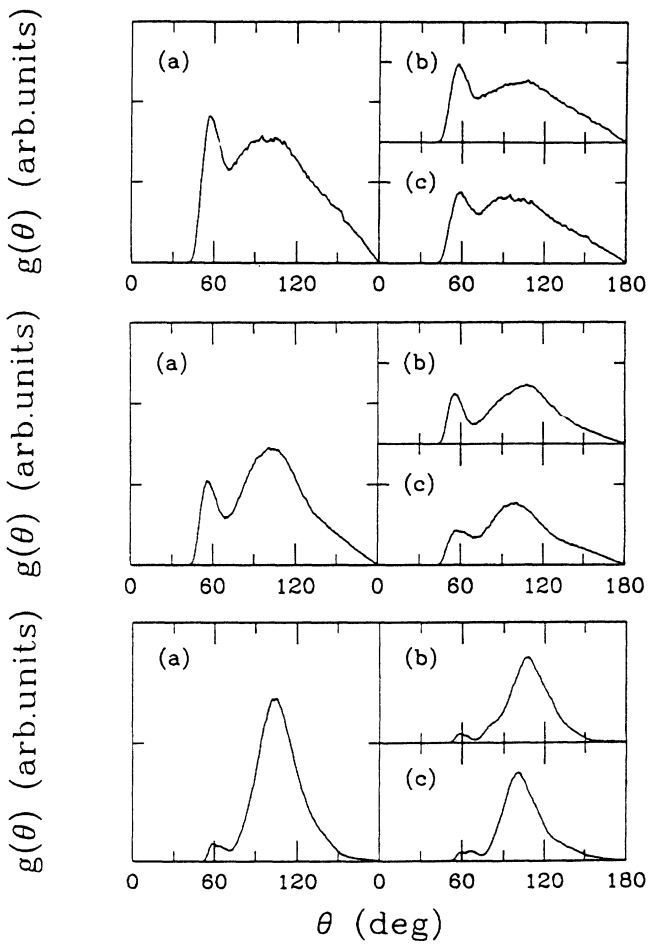

FIG. 3. Total and partial bond angle distributions for GaAs at 1600 K (l-GaAs, top panel), at 800 K (center panel), and at 300 K (a-GaAs, bottom panel); (a) total; (b) X-Ga-X; (c) X-As-X.

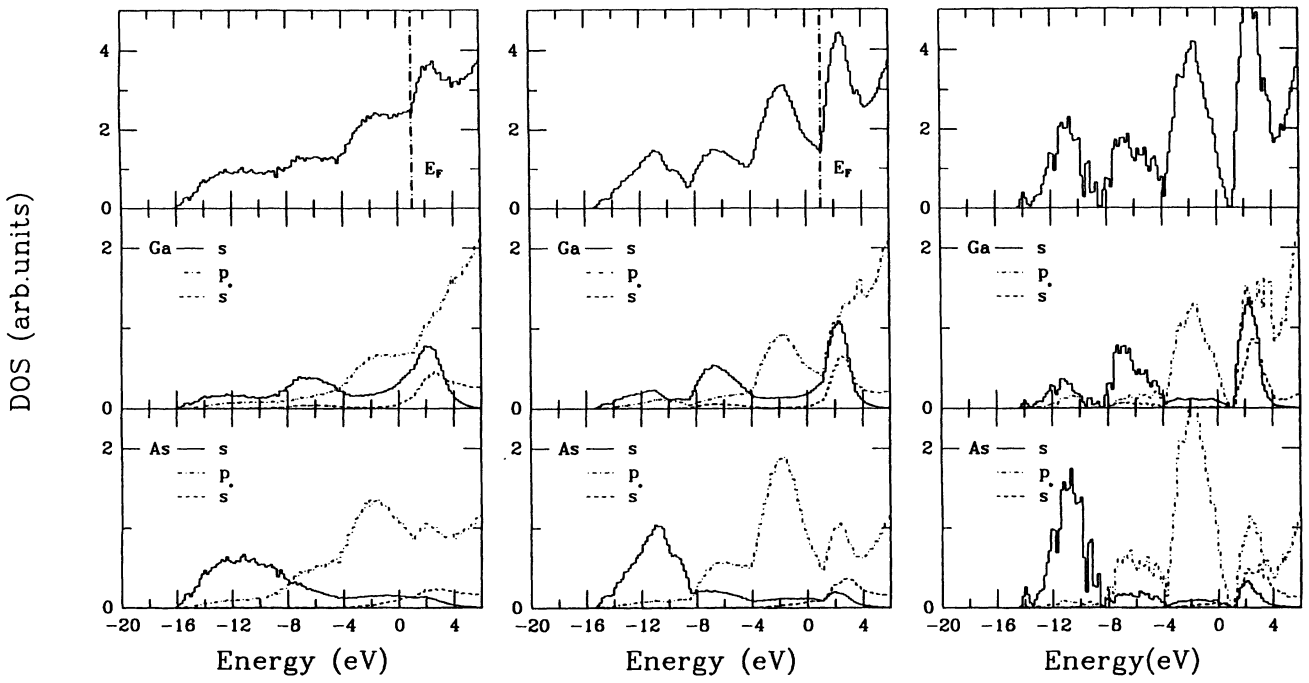

FIG. 4. Electronic densities of states (top), and their cationic (middle) and anionic (bottom) contributions, projected on s, p, and s^* states for GaAs at 1600 K (l-GaAs, left), at 800 K (center), and at 300 K (a-GaAs, right). The dash-dotted line in the top panel indicates the Fermi level.

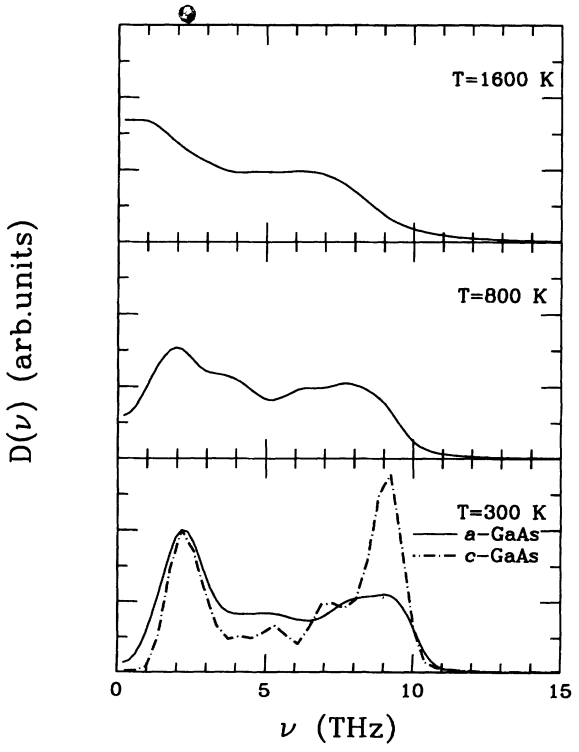

FIG. 5. Vibrational density of states for GaAs at 1600 K (l-GaAs, top panel), at 800 K (center panel), and at 300 K [bottom panel; a-GaAs (solid line) and c-GaAs dash-dotted line].

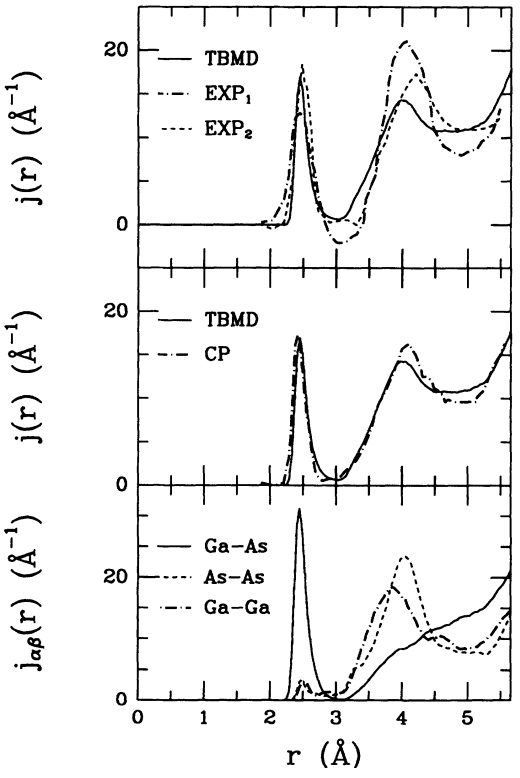

FIG. 6. Total [$j(r)$] and partial [$j_{\alpha\beta}(r)$] radial distribution functions for a-GaAs at 300 K. Comparisons with experimental [EXP_1, x-ray diffraction data (Ref. 1); EXP_2, electron diffraction data (Ref. 2)] and *ab initio* (Ref. 9) (*CP*) results are shown in the top and center panels, respectively.

TABLE III. Partial coordination numbers in a-GaAs for different cutoff distance (d_{1NN}).

	X-X	Ga-X	As-X	Ga-As	As-Ga	Ga-Ga	As-As
TBMD (d_{1NN}=2.8 Å)	3.925	3.92	3.93	3.55	3.55	0.37	0.38
TBMD (d_{1NN}=3.0 Å)	4.09	4.09	4.09	3.83	3.83	0.53	0.53
CP (Ref. 9)	3.83	3.83	3.83	3.45	3.45	0.38	0.38
Expt. (Ref. 5)	3.93						

Fig. 3 [bottom panel (b) and (c)], where the $g_{X\text{-}Y\text{-}X}(\theta)$ (X, Y=Ga,As) are reported. Only minor differences have been observed with respect to the total one (a): this clearly indicates that a-GaAs has a nonrandom chemical structure and the tetrahedral coordination is dominant. We note that the maximum of $g(\theta)$ is systematically shifted towards lower angles when the pivot atom is As.

The overall structural features of our computer-generated sample are summarized in the total and partial radial distribution functions [$j(r)$ and $j_{\alpha\beta}(r)$, respectively] as reported in Fig. 6, where the experimental[1,2] and *ab initio*[9] $j(r)$ are also shown. The agreement looks quite good for both the position of the first and second peaks and for the absolute intensity of the total $j(r)$. Even the onset of $j(r)$ and the width of the gap between its first and second maximum are pretty well reproduced. This suggests that both the fraction and the spatial distribution of the empty space surrounding each atom are correctly described in the present simulation.

As for the chemical order of a-GaAs, useful information can be obtained from Fig. 2 (bottom panel) and by calculating the relative occurrence of point defects (Table IV). We have found a sizable amount of threefold-coordinated (C_3) sites, at a concentration rate that varies according to the cutoff distance for 1NN (d_{1NN}). The large amount of C_3 atoms, when compared to the case of a-Si, where they have been found not to exceed the 4–5%,[4] is consistent with the structural model by O'Reilly and Robertson,[7] where C_3 atoms are indicated as more stable in a-GaAs than in elemental amorphous semiconductors. The second important feature of Table IV is the presence of fivefold-coordinated (C_5) sites. This result is in contrast with the first-principles simulation of Ref. 9 where no C_5 atoms were found. We believe that such a disagreement is originated by the artificial switches of Ga to As, which has been introduced in Ref. 9.

Another important issue that characterizes the amount of chemical order in a-GaAs is the fraction of wrong bonds, i.e., bonds linking like atoms. The qualitative picture derived from experiments[1–6] indicates that such wrong bonds are indeed present in a-GaAs, still at low concentration. Estimations range from a few percent up to 12%. This feature is confirmed by first-principles simulations,[9] where a 10% fraction of wrong bonds was found at 300 K. This result, however, is again dependent on the artificial AsGa switches operated at T=800 K, in order to reduce the large number of wrong bonds found at that temperature. Actually, they were found to be 21% after the quenching from 1600 K. Thanks to these switches, the fraction of the like-atom bond was reduced

TABLE IV. Occurrence of point defect in a-GaAs.

	C_3 (%)	C_4 (%)	C_5 (%)	Wrong bonds (%)
TBMD (d_{1NN}=2.8 Å)	17	73	10	9.5
TBMD (d_{1NN}=3.0 Å)	14	66	18	
CP (Ref. 9)	21	79		10
Expt. (Ref. 5)				12

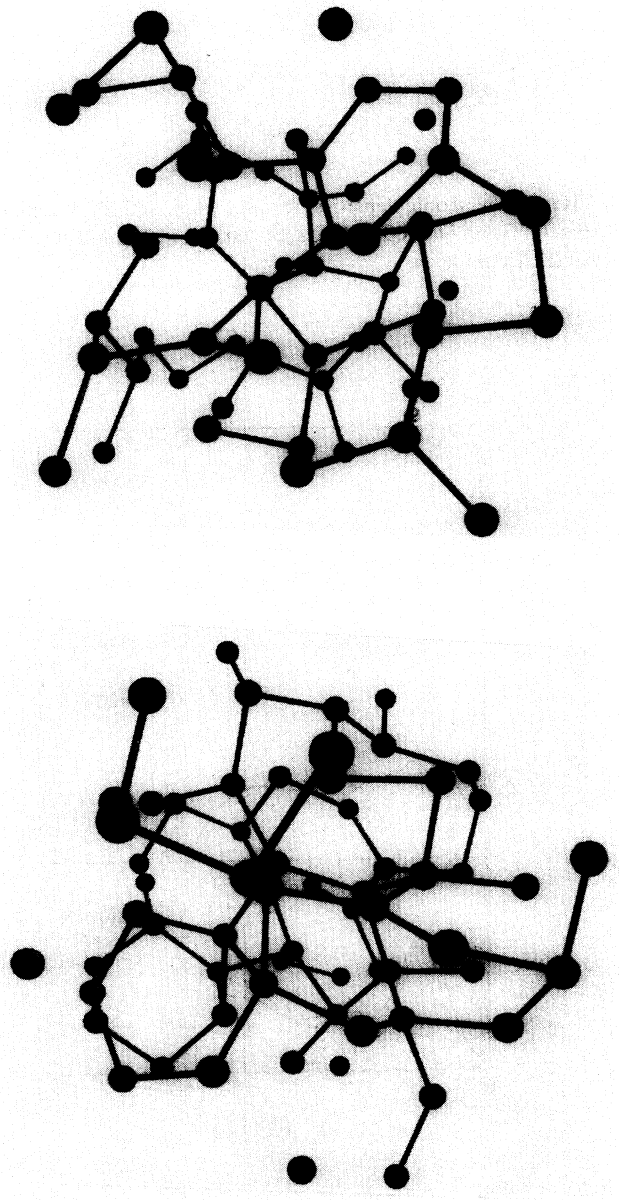

FIG. 7. Atomic configurations of the a-GaAs sample at the end of the observation period.

in Ref. 9 to 12–13 % and finally to 10%, after the last cooling down to 300 K. On the contrary, in our simulation, the fraction of wrong bonds has been found to be ~15% at 800 K and 12.9% at room temperature. This result is in good agreement with the available experimental data[1–6] and indicates that the atomic diffusion in the 1600–800-K temperature range is the main feature governing the ordering process into the sample.

The cation and anion coordination numbers (Table III) are very similar and this confirms the picture of a chemically ordered amorphous network. On the other hand, Ga atoms form more easily C_3 sites with As atoms than vice versa.

So far we have considered only the structural features of *a*-GaAs. We have also calculated both the electronic and vibrational DOS in order to get a deeper insight into the present structural model. In Fig. 4 (right) we display the total electronic DOS (top panel) and the Ga-projected and As-projected DOS (middle and lower panels, respectively). The integration over the Brillouin zone has been limited to (000) point of the simulation supercell, while the DOS has been obtained through a temporal average on the observation time. The main feature of the electronic DOS are in rather good agreement to the experimental valence x-ray-photoelectron-spectroscopy data,[6] where three main structures at ~ −2, ~ −6, and ~ −11 eV were observed. In particular, we have reproduced the low-energy gap close to −8 eV separating the two *s*-like bands and the important semiconductive gap between valence and conduction bands.

As for the vibrational spectrum, it is reported in Fig. 5 (bottom panel), where the total vibrational DOS $D(\nu)$ of both *a*-GaAs (full line)[25] and crystalline GaAs (*c*-GaAs; dash-dotted line) are reported. In both cases, they have been estimated at 300 K, starting from a well-equilibrated sample. The $D(\nu)$ has been calculated from the Fourier transformed velocity-velocity autocorrelation function collected during a 5-ps run with a time step as large as 10^{-15} s. The part of the vibrational spectrum falling in the acoustic region ($\nu < 5$ THz) is nearly unchanged when passing from *a*-GaAs to *c*-GaAs, as should be expected since the average coordination of *a*-GaAs is mainly tetrahedrallike. On the other hand, the optical region shows important changes from crystalline to the amorphous phase. The strong peak at ~9 THz as related to longitudinal optical vibrations of *c*-GaAs, and its low-frequency shoulder at ~7 THz have merged into one broad structure. This is a clear fingerprint of the *local* structural disorder of the amorphous network that is particularly well depicted by the real-space image reported in Fig. 7. In fact, as previously discussed, both bond length and bond angle are locally distorted and the corresponding frequency of the stretching and bending vibrational modes are likely to be affected.

ACKNOWLEDGMENTS

Professor J. Skofronick (Florida State University, Tallahassee, FL) and the Supercomputer Computation Research Institute (SCRI, Tallahassee, FL) are greatly acknowledged for computational support.

[1] N. J. Shevchik and W. Paul, J. Non-Cryst. Solids **13**, 1 (1973).
[2] A. Gheorghiu, K. Driss-Khodja, S. Fisson, M. L. Theye, and J. Dixmier, J. Phys. (Paris) Colloq. **46**, C8-545 (1985).
[3] R. J. Temkin, Solid State Commun. **15**, 1325 (1974).
[4] M. L. Theye, A. Gheorghiu, and H. Launois, J. Phys. C **13**, 6569 (1980).
[5] N. J. Shevchik, J. Tejeda, and M. Cardona, Phys. Rev. B **9**, 2627 (1974).
[6] C. Senemaud, E. Belin, A. Gheorghiu, and M. L. Theye, Solid State Commun. **55**, 947 (1985).
[7] E. P. O'Reilly and J. Robertson, Phys. Rev. B **34**, 8684 (1986).
[8] S. T. Pantelides, Phys. Rev. Lett. **57**, 2979 (1986).
[9] E. Fois, A. Selloni, G. Pastore, Q. M. Zhang, and R. Car, Phys. Rev. B **45**, 13 378 (1992).
[10] C. Molteni, L. Colombo, and L. Miglio, Europhys. Lett. **24**, 659 (1993); (unpublished).
[11] L. Goodwin, A. J. Skinner, and D. G. Pettifor, Europhys. Lett. **9**, 701 (1989); C. Z. Wang, C. T. Chan, and K. M. Ho, Phys. Rev. B **39**, 8586 (1989).
[12] R. Virkkunen, K. Laasonen, and R. M. Nieminen, J. Phys. Condens. Matter **3**, 7455 (1991).
[13] C. Z. Wang, C. T. Chan, and K. M. Ho, Phys. Rev. B **45**, 12 227 (1992).
[14] G. Servalli and L. Colombo, Europhys. Lett. **22**, 107 (1993).
[15] D. Maric and L. Colombo, in *Crystallization and Related Phenomena in Amorphous Materials—Ceramics, Metals Polymers, and Semiconductors,* edited by M. Libera, T. E. Haynes, P. Cebe, and J. Dickinson, MRS Symposium Proceedings No. 321 (Material Research Society, Pittsburgh, 1994).
[16] Q. M. Zhang, G. Chiarotti, A. Selloni, R. Car, and M. Parrinello, Phys. Rev. B **42**, 5071 (1990).
[17] C. Bergman, C. Bichara, P. Chieux, and J. P. Gaspard, J. Phys. (Paris) Colloq. **46**, C8-97 (1986).
[18] D. J. Chadi, Phys. Rev. B **29**, 785 (1984).
[19] W. A. Harrison, *Electronic Structure and Properties of Solids* (Freeman, San Francisco, 1980).
[20] P. Vogl, H. P. Hjalmarson, and J. D. Dow, J. Phys. Chem. Solids **44**, 365 (1983).
[21] J. A. Majewski and P. Vogl, *The Structure of Binary Compounds* (North-Holland, Amsterdam, 1989), p. 287.
[22] S. Froyen and M. Cohen, Phys. Rev. B **28**, 3258 (1983).
[23] P. C. Kelires and J. Tersoff, Phys. Rev. Lett. **63**, 1164 (1989).
[24] C. Molteni, L. Colombo, and L. Miglio, in *Materials Synthesis and Processing Using Ion Beams,* edited by R. J. Culbertson, K. S. Jones, O. W. Holland, and K. Maex, MRS Symposia Proceedings No. 316 (Materials Research Society, Pittsburgh, 1994).
[25] Note that no macroscopic field is included in our calculations, so that no LO-TO splitting is present.

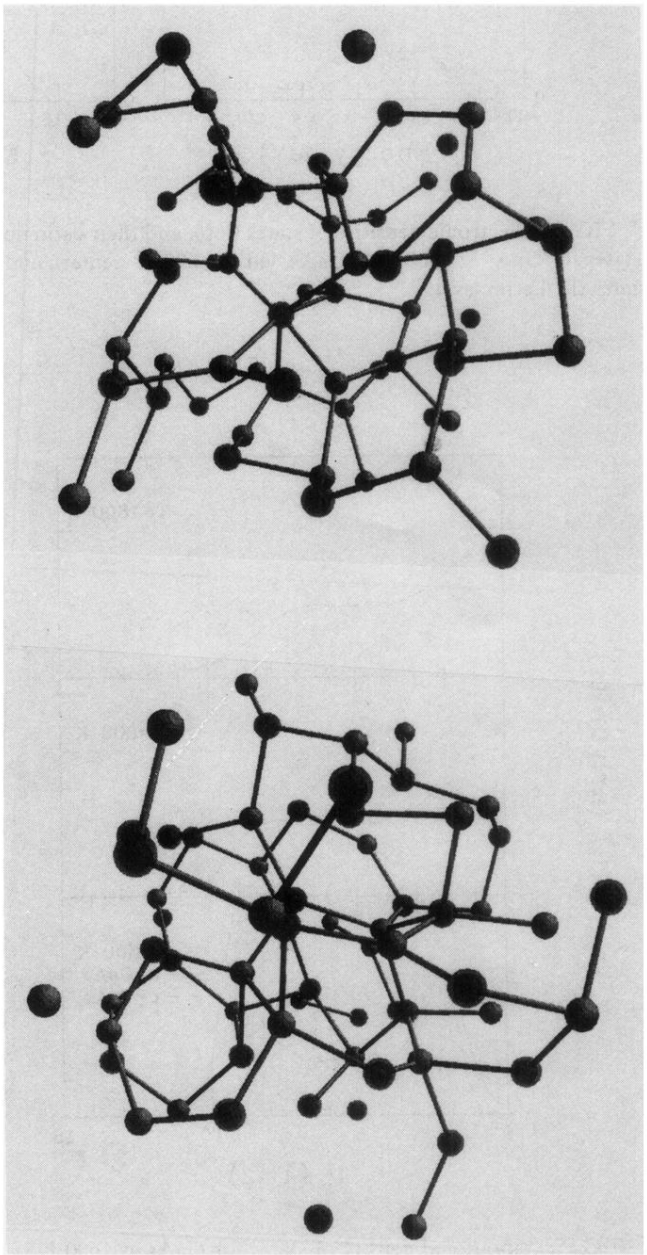

FIG. 7. Atomic configurations of the *a*-GaAs sample at the end of the observation period.